Through-pore polymerization in polar high-performance liquid chromatography columns allowing scanning electron microscopy based imaging of the packing order

Hou, Zhanyao; Broeckhoven, Ken; Desmet, Gert; Lynen, Frederic

Published in:
Journal of Chromatography A

DOI:
10.1016/j.chroma.2020.461851

Publication date:
2021

License:
CC BY-NC-ND

Document Version:
Accepted author manuscript

Highlights

- A new in-column methacrylate-based polymerization procedure was developed for imaging the internal morphology of bare silica HPLC columns
- Polymerization was performed in a commercial and in a home-made silica column
- The obtained silica/polymeric rod can be mechanically cut allowing cross section SEM imaging
- The developed procedure allows mapping of the local external porosity in packed column
- The procedure could be of assistance to steer the optimization of packing processes of HPLC columns.

Through-pore polymerization in polar high-performance liquid chromatography columns allowing scanning electron microscopy based imaging of the packing order

Zhanyao Hou[a], Ken Broeckhoven[b], Gert Desmet[b], Frederic Lynen[a]*

a. Separation Science Group, Department of Organic and Macromolecular Chemistry, Faculty of Sciences, Ghent University, Krijgslaan 281-S4 Bis, B-9000 Ghent, Belgium.

b. Vrije Universiteit Brussel, Department of Chemical Engineering, Pleinlaan 2, Brussel, Belgium.

*Corresponding Author.

Tel: +32 (0) 9 264 9606; Fax: +32 (0) 9 264 4998. E-mail: frederic.lynen@ugent.be (F. Lynen)

Abstract

To allow an enhanced understanding of the order in packed HPLC columns, in this work a methodology for immobilizing native polar silica particles is developed based on the polymerization of a methyl methacrylate (MMA) and ethylene glycol dimethacrylate (EGDMA) as a cross-linker in the interstitial pores of HPLC columns. Subsequent mechanical cutting then allows scanning electron microscopy (SEM) based imagery of cross-sections of the packed bed. In this way, the packing efficiency of home-made and commercial HPLC columns with 4.6 mm inner diameter and 150 mm length comprising the same packing material of 5 µm silica particles are compared. The methodology is developed for native silica used in e.g. hydrophilic interaction liquid chromatography (HILIC) and in normal phase LC. In order to confirm the feasibility of the developed methodology, the conventional methods for the evaluation of column, efficiency and porosity, are also employed. The obtained porosity information is compared and showed the same trend with the external porosity measurements obtained *via* inverse size exclusion approach, illustrating its potential application to study the micro-heterogeneity of packed HPLC columns and to guide the optimization of the packing process of HPLC columns.

Keywords

HPLC
HILIC
Packing quality
SEM imaging
External porosity
Through pores

1. Introduction

Column technology in liquid chromatography has been continually evolving over the last decades driven by the never-ending pursuit for faster and more efficient analyses. In packed column LC this resulted in the use of more homogenously shaped and of systematically smaller particles. [1-5] The advent of ultra-high-performance LC (UHPLC) made it possible to use sub-2 micron sized particles allowing columns to generate more plates per unit of time and operation well above their optimal velocity. More recently the now broad implementation of the (old) concept of core-shell particle technology in (U)HPLC has led to further improvements in plate height, or for mitigation of the demanding pressure requirements involved. [6-11]

While the rule of thumb relationships between particle size and obtained plate heights and column efficiencies are well-known, whereby for fully porous particles reduced plate heights (h) ≈2 are expected, this neglects the non-negligible influence of the micro-heterogeneity of packed beds, whereby the packing density locally differs in the column (both over the longitudinal and radial axis of the column) depending on the packing conditions. This results e.g. in observations that the bottom sections of packed columns (hence the column outlet) allow obtaining more efficient separations [12]. Alternatively, parallel segmented flow chromatography work, whereby the effluent close to the column wall is discarded (while preserving the central flow region) have demonstrated that plate height improvements can be obtained when being able to avoid wall effects. On the other hand, the higher order obtained in lithographically manufactured pillar array nano/micro-LC columns has shown that it is possible to reach h≈0.8-1 values. Such observations illustrate that the current accepted reduced plate height limit ≈2.0 is an average value which might still be somewhat improved with increased understanding (or optimal exploitation) of the column heterogeneity. The latter, which can be of relevance in the development of enhanced packing processes, can be accessed via imaging approaches allowing reconstruction of the internal order in HPLC columns. [13]
A number of strategies towards the physical reconstruction by direct imaging of packed beds have been developed based on electron tomography [14], micro-X-ray computerized tomography [15, 16], visual monitoring of elution bands in glass columns [17, 18], focused ion-beam scanning electron microscopy [16, 19-21] and nuclear magnetic resonance imaging[22-24]. Detailed work have thereby been performed by Tallarek et al. on e.g. the reconstruction of packed bed structures in capillary columns.[19, 20, 25-27] The information obtained via such techniques provides insight into the relationship between the morphological properties of packed beds and their performance. In this way e.g. the influence of slurry concentration during the packing process on the formation of larger voids and wall-effects was studied, whereby the results revealed that increasing of the slurry density counteracts these detrimental phenomena [26].

Thus far, most interest in terms of 3D reconstruction of packed beds focused on capillary columns through direct imaging approaches.[25, 27-30] To the best of our knowledge, only one morphological study of the packed bed in analytical stainless steel column (2.1 x 50 mm) has been reported so far, in which the wall-effects of reversed phase liquid chromatography (RPLC) were investigated in conventional stainless steel packed columns.[19] This approach comprised the in-column polymerization of styrene and divinylbenzene allowing extrusion of the packed bed and slicing for subsequent focused ion-beam scanning electron microscopy. In the present report, we propose an in-column polymerization approach based on methyl methacrylate (MMA) and ethylene glycol dimethacrylate (EGDMA). The methodology allows evaluation of the packing quality in (4.6 x 150 mm) columns comprising polar stationary phases used in hydrophilic interaction (HILIC) or normal phase LC (NPLC). After polymerization and mechanical cutting, scanning electron microscopy (SEM) imaging is performed of cross-sections of the packed bed. The obtained SEM, column performance and porosity data of an unaltered commercial column and of a repacked column are compared and discussed.

2. Materials and methods

2.1 Chemicals and reagents

HPLC grade acetonitrile (ACN), 2-propanol, *N,N*-dimethylformamide(DMF), dichloromethane (DCM), tetrahydrofuran (THF), methyl methacrylate (MMA), ethylene glycol dimethacrylate (EGDMA), 2,2'-azobis(isobutyronitrile) (AIBN) (98%) and all test solutes (thymine, adenine,

guanine) were obtained from Sigma-Aldrich (Steinheim, Germany) and used as received, unless otherwise stated. Acenaphthene originated from Merck (Hohenbrunn, Germany). Milli-Q grade water (18.2 mΩ) was purified and deionized in-house by a Milli-Q plus instrument from Millipore (Bedford NH, USA). MMA and EGDMA were passed over a basic aluminum oxide column to remove the inhibitor before use (the structures are shown in Scheme S1). AIBN was recrystallized from methanol two times before use. ZORBAX Rx-SIL (4.6 x 150 mm, 5 µm, 80 Å) pure silica columns were purchased from Agilent Technologies (Brussels, Belgium). For the home-made column, the same Rx-SIL material was repacked into 150 x 4.6 mm ID stainless-steel columns obtained from IDEX Health & Science (Middleborough, MA, USA). Polystyrene standards with 12 different molecular weights ranging between 500 Da and 2000 K Da were used for inverse size exclusion chromatography (ISEC) experiments and were also purchased from Sigma-Aldrich.

2.2 Sample preparation

Stock solutions of thymine and adenine were prepared in a concentration of 1000 ppm in H_2O. Acenaphthene and guanine were dissolved separately at a concentration of 1000 ppm in acetonitrile and 0.1 M NaOH, respectively. Fresh test samples consisting of 100 ppm acenaphthene, 80 ppm thymine, 100 ppm adenine and 100 guanine were prepared daily by mixing and diluting the stock solutions in acetonitrile for the evaluation of the column performance.
Stock ammonium formate solutions were prepared by dissolving the appropriate amount of ammonium formate in water and adjusting to pH=6.4 by formic acid. The concentration of the former in the total mobile phase was kept constant at 10 mM for all HILIC analyses.

2.3 Instrumentation

Chromatographic data were acquired with an HPLC Agilent 1100 system (Agilent Technologies, Waldbronn, Germany). The maximum operating pressure of the system was 400 Bar. This instrument includes an auto-sampler, a variable wavelength UV detector equipped with a 2 µl micro-flow cell and a column oven. Data acquisition, data handling, and instrument control were performed using Chemstation software (Agilent). Between the injector and the inlet of the column and between the outlet of the column and the detector, (120 µm I.D.) stainless steel connections of 400 mm and 280 mm in length were used, respectively. These were not altered during the experiments to avoid changing the extra-column volume. During all HPLC experiments detection was performed at 254 nm. The microstructure of the packed beds was analyzed by a scanning electron microscopy (SEM, FEI Quanta 200F, FEI Europe B.V., Netherlands). Prior to SEM analysis, a gold coating was applied to the samples using a sputter coater (Balzers Union SKD030, Oerlikon Balzers Coating Benelux N.V., Belgium).

2.4 Methods

2.4.1 Column packing procedure

The silica particles for the home-made column were obtained by unpacking two ZORBAX RX-SIL columns. The 150 x 4.6 mm ID stainless steel column were slurry-packed with methanol by a Haskel air-driven pump (Burbank, CA, USA). For the slurry, 2.5 g silica was suspended in 20 mL methanol. The column was packed at 900 Bar for 40 min. After packing, the columns were conditioned with water and ACN until a stable UV signal.

2.4.2 Column efficiency and porosity assessments

These result are given in the Supplementary Materials (S2-S6).

2.4.3 Methodology for immobilization of silica particles and SEM imaging

For the reconstruction of the micro-morphology of the beds of the two columns, the silica particles were immobilized by the in-column cross-linked polymerization of MMA and EGDMA by the following procedure. The stock polymerization solution was prepared by dissolving MMA (15.9 mL, 0.15 mol), EGDMA (84.9 mL, 0.45 mol) and AIBN (4.9 g, 0.03 mol) in 257.6 mL DMF. Prior to

the filling polymerization solution into columns, the solution was purged with nitrogen for 20 min to remove residual oxygen. During the filling of the polymerization solution in columns, the solution was continuously purged by nitrogen. The filling process was performed by LKB Bromma 2248 HPLC pump for 120 min at 0.5 mL/min. Afterwards, the columns were disconnected, sealed and placed at 50 °C in an oven. After 4 hours, the oven was raised to 70 °C in 5 hours, maintained at 70 °C overnight (ca. 15 h). In order to obtain the identical cross-linked polymer structure, the two columns were filled with the same polymerization solution and placed in the oven at the same time. After the process, the temperature of the oven was slowly lowered back to room temperature. After reaching room temperature, the silica/polymer rod of immobilized silica particles was extruded from its steel housing by the column packing system. An image of the obtained silica/polymer rod after extrusion (the home-made column as an example) is shown in Figure 1 (A). Small pieces were cut from the extruded rod by mechanical cross sectioning. The cross-sections of samples for SEM measurement were prepared by "potting" of the samples whereby the sample is embedded in an epoxy resin, following by grinding and polishing to the plane of interest. (Fig. 1B). To increase the sample conductivity, a thin gold layer was subsequently deposited onto the sample surfaces. The SEM images were captured in the bulk central region of cross-section to avoid the occurrence of wall effects (Fig. 1C).

Figure 1

2.4.4 Methodology for image process and analysis

The processing of the SEM images was performed with the Adobe Photoshop CS3 extended and ImageJ (1.52a) software. The former was used for cropping the SEM data into equal sized 30 µm x 30 µm square images whereby the areas occupied by the silica was highlighted in black to increase the contrast between silica and polymer areas. Subsequently the resulting image was opened by ImageJ allowing adjusting the area covered by the polymer to white and for conversion to binary data leading to the determination of the percentage of space occupied by the silica.

3. Results and discussion.

In this work, a new in-column polymerization approach is proposed allowing studying the microstructure of columns packed with polar stationary phases (used e.g. in hydrophilic interaction or normal phase LC). Three identical commercial columns were used, whereby two were unpacked to collect the material. One column was subsequently repacked to allow studying the influence of the packing process on the local packing density. In this study, the performance and porosity of the columns is first assessed to allow subsequent enhanced interpretation of the microstructure information obtained via the SEM imaging.

A HILIC mobile phase and test sample allowing obtaining, on a well packed column, satisfactory retention and symmetric peak shapes under isocratic conditions was used for this purpose.[31] A representative chromatogram obtained in this way on both columns is shown in Figure 2.

Figure 2

When comparing both chromatograms and the data reported in the supplementary information, significant differences appear, whereby the repacked column is characterized by asymmetric peaks and reduced retention compared to what can be observed on the commercial column (Table S1). In order to assess this in more detail, the corresponding van Deemter plots were constructed as shown in Figure S1. This data (also represented in numerical format in Table S2 confirms that the home-made column is performing systematically worse and that reduced place heights of ~2.4 were obtained compared to ~1.9 on the commercial column for both most retained analytes.

In order to corroborate if this information points towards the occurrence of a less densely packed bed in the home-made column, porosity measurements were also performed on both columns. The total porosity (ε_T) refers to the fraction of the total volume of mobile phase in a HPLC column. The total porosity can be split into two different contributions, external porosity (ε_e) and internal porosity (ε_{int}). The external porosity is the column volume that is not occupied by the particles, relative to the column geometrical volume. The internal porosity stems from the void space inside of the particles. The total porosity values were determined *via* the void times of the unretained t_0-

marker (Acenaphthene) during the van Deemter experiments (VD) and *via* pycnometry (table 1). The origin of the differences in total porosity between both approaches has been well described in literature.[32] This is e.g. related to the challenge to find a truly unretained solute which is able to diffuse even into the deepest pores. It is thereby interesting to observe that a slightly higher total porosity is measured on the commercial column with both techniques.

Table 1

While the total porosity is not allowing for much insight into the quality of a packed bed, the external porosity (ε_e) does provide more information as it represents the amount of unoccupied space in a column. In this work, the external porosity was determined by inversed size exclusion (ISEC) experiments under two conditions (at two different flow rates) of which the corresponding data is represented in Table 1 (and Figure S2). This reveals a larger external porosity for the home-made column. This corresponds well with the column performance information. On the one hand a less dense packed structure implies there is a larger variation between densely packed and less densely packed regions, resulting in a more tortuous path followed by the analytes when migrating through the bed, and hence to an increased A-term. On the other hand, a larger ε_e also causes an increase in the average diffusional distances and leads to a less efficient mass transfer and hence to a steeper C-term.

While the external porosity allows indeed for a reflection of the packing quality of a column, it only provides an average value. This can be considered a crude approach as it is difficult to relate to the packing conditions and to the microstructure in the column. Therefore, a cross-linked polymerization approach was developed allowing in-column immobilization of the individual silica particles. The used polymerization conditions were firstly optimized in conventional glassware (hence not in-column). This approach allows optimization of the choice of monomer, the ratio of monomer to cross-linker, and the solvent ratio's. For maximal compatibility with the polar silica, the methodology was developed with the rather polar methyl methacrylate (MMA) and ethylene glycol dimethacrylate (EGDMA) whereby the DMF was used as a solvent depicting the ability to sufficiently "wet" the silica. The high reactivity and fast reaction kinetics of methacrylates were thereby also considered essential to allow complete filling of the through pores of columns. With a MMA/EGDMA (1/3, mol/mol) in 30% DMF (relative to the weight of total polymerization solution) relatively rigid polymeric cross-linked structures were obtained. To avoid the occurrence of fissures in the obtained cross-linked structures, it proved most effective to allow the polymerization to occur in the first 4 hour of the process at 50°C. This minimized the polymer shrinkage phenomenon occurring upon the fast polymerization. The polymerization can then be completed by subsequently raising the temperature to 70°C and maintaining it there for 15 hours. The process was finalized through a controlled slow cooling to room temperature. The in-column polymerization was performed under these optimized conditions whereby the degassed stock polymerization solution was filled into the column at 0.5 ml/min for 120 min. The filling solution and the columns where thereby cooled in an ice bath to prevent polymerization already occurring during the filling procedure. After the in-column polymerization, the material was extruded from the columns and the samples for SEM analysis were prepared as discussed in the Supporting Information.

To investigate whether the quality of a packed bed relates to a higher packing density, the proportion of silica visible in regions of identical size in column cross-sections were compared between the home-made and commercial columns. These cross-sections were polished to homogenize the surfaces and to make the counting of the proportion of silica possible (See Figure S3 for an example of a SEM image of an unpolished and a polished surface). Note that the silica in the obtained silica/polymer rod can be leached out under strongly basic conditions. However, this was not performed for the SEM imaging, as the contrast between the silica and the polymer proved high enough for differentiation of both zones, while allowing insight into the original micro-morphology in the best way.

The developed methodology provides the observed (local) external porosity information,[19, 33] to obtain the averaged data, the SEM samples were cut randomly from the extrusion rod. All SEM images were acquired from the center of the cross-section of each sample to avoid the wall effects inevitably occurring in any packed bed packing. The randomness of the packing structure of silica particles is visible in figure S3 (and in the other SEM images below), whereby the occasional missing of a silica particle due to the mechanical polishing can easily be ascertained. To calculate the proportion of silica in cross-section, the SEM images were processed following the procedures

stated in the Materials and Method section (Section 2.4.4 and Figure S4).

For each column, four 30 µm x 30 µm square images were cropped randomly and processed to analyze the proportion of silica (Figure 3). Table 2 summarizes the % proportions of silica in each image together with the averaged values and deviations in each column. The higher packing density of the commercial compared to the home-made column is thereby reflected through the larger percentage of occupied space by the silica in all micrographs. This data can e.g. be converted into the observed (local) external porosity values (ε_{e_local} = 1-Si%) included in Table 1. Interestingly, lower variations in silica coverage (expressed in RSD%) are observed on the commercial column, which therefore also appears to be a characteristic reflecting more homogeneously packed beds.

Figure 3

Table 2

Hence the average polymer proportion in the two-dimensional cross-section can be regarded to reflect the percentage thereof in the three-dimensional extrusion rod. The local or, alternatively the average external porosity, are thereby obtained from processing of individual (parts of) SEM images or by averaging the data over multiple images, respectively.

4. Conclusion

In this study, a new approach was developed to polymerize the through pores in HPLC columns packed with polar particles. Methyl methacrylate (MMA) and ethylene glycol dimethacrylate (EGDMA) are thereby polymerized in a 1/3 ratio in native silica columns. After this process, the immobilized particles in the formed polymer can be easily extruded, mechanically cut and polished for subsequent scanning electron microscopy based imagery. The methodology was used on a commercial and on a homemade column packed with the same stationary phase. The obtained porosity information follows the same trend as obtained via inversed size exclusion chromatography, illustrating its potential to study the micro-heterogeneity of packed HPLC columns. The procedure could be of assistance to steer the optimization of packing processes of HPLC columns.

Acknowledgements

Z.H. acknowledges the Research Foundation-Flanders (FWO) for funding part of this research (grant G0D0218N). The FWO and the FNRS are acknowledged for funding part of this research through the Excellence of Science grant (30897864). BOF-Ugent is also acknowledged for co-funding this work (grant 01J15417). We acknowledge support by the UGent Expertise Center for Nano- and Microfabrication - NaMiFab for preparing the cross-sections. Kim Vanderlinden (Vrije Universiteit Brussel, Department of Chemical Engineering) is thanked for help with the initial tests of the polymerization method.

References

[1] G. Cancelliere, A. Ciogli, I. D'Acquarica, F. Gasparrini, J. Kocergin, D. Misiti, M. Pierini, H. Ritchie, P. Simone, C. Villani, Transition from enantioselective high performance to ultra-high performance liquid chromatography: A case study of a brush-type chiral stationary phase based on sub-5-micron to sub-2-micron silica particles, Journal of Chromatography A, 1217 (2010) 990-999.

[2] G. Desmet, D. Clicq, D.T.T. Nguyen, D. Guillarme, S. Rudaz, J.-L. Veuthey, N. Vervoort, G. Torok, D. Cabooter, P. Gzil, Practical Constraints in the Kinetic Plot Representation of Chromatographic Performance Data: Theory and Application to Experimental Data, Analytical Chemistry, 78 (2006) 2150-2162.

[3] P.W. Carr, X. Wang, D.R. Stoll, Effect of Pressure, Particle Size, and Time on Optimizing Performance in Liquid Chromatography, Analytical Chemistry, 81 (2009) 5342-5353.

[4] D. Cabooter, J. Billen, H. Terryn, F. Lynen, P. Sandra, G. Desmet, Kinetic plot and particle size distribution analysis to discuss the performance limits of sub-2µm and supra-2µm particle columns, Journal of Chromatography A, 1204 (2008) 1-10.

[5] A. de Villiers, F. Lestremau, R. Szucs, S. Gélébart, F. David, P. Sandra, Evaluation of ultra performance liquid chromatography: Part I. Possibilities and limitations, Journal of Chromatography A, 1127 (2006) 60-69.

[6] J.J. Salisbury, Fused-Core Particles: A Practical Alternative to Sub-2 Micron Particles, Journal of Chromatographic Science, 46 (2008) 883-886.
[7] F. Gritti, G. Guiochon, Theoretical investigation of diffusion along columns packed with fully and superficially porous particles, Journal of Chromatography A, 1218 (2011) 3476-3488.
[8] F. Gritti, G. Guiochon, Diffusion models in chromatographic columns packed with fully and superficially porous particles, Chemical Engineering Science, 66 (2011) 3773-3781.
[9] K. Horváth, F. Gritti, J.N. Fairchild, G. Guiochon, On the optimization of the shell thickness of superficially porous particles, Journal of Chromatography A, 1217 (2010) 6373-6381.
[10] D.A. Spudeit, M.D. Dolzan, Z.S. Breitbach, W.E. Barber, G.A. Micke, D.W. Armstrong, Superficially porous particles vs. fully porous particles for bonded high performance liquid chromatographic chiral stationary phases: Isopropyl cyclofructan 6, Journal of Chromatography A, 1363 (2014) 89-95.
[11] K. Broeckhoven, D. Cabooter, G. Desmet, Kinetic performance comparison of fully and superficially porous particles with sizes ranging between 2.7μm and 5μm: Intrinsic evaluation and application to a pharmaceutical test compound, Journal of Pharmaceutical Analysis, 3 (2013) 313-323.
[12] F. Gritti, G. Guiochon, Effect of parallel segmented flow chromatography on the height equivalent to a theoretical plate. I—Performance of 4.6mm×30mm columns packed with 3.0μm Hypurity-C18 fully porous particles, Journal of Chromatography A, 1297 (2013) 64-76.
[13] S. Jespers, S. Schlautmann, H. Gardeniers, W. De Malsche, F. Lynen, G. Desmet, Chip-Based Multicapillary Column with Maximal Interconnectivity to Combine Maximum Efficiency and Maximum Loadability, Analytical Chemistry, 89 (2017) 11605-11613.
[14] J.F. Langford, M.R. Schure, Y. Yao, S.F. Maloney, A.M. Lenhoff, Effects of pore structure and molecular size on diffusion in chromatographic adsorbents, Journal of Chromatography A, 1126 (2006) 95-106.
[15] C.J. Gommes, A.-J. Bons, S. Blacher, J.H. Dunsmuir, A.H. Tsou, Practical methods for measuring the tortuosity of porous materials from binary or gray-tone tomographic reconstructions, AIChE Journal, 55 (2009) 2000-2012.
[16] T.F. Johnson, F. Iacoviello, D.J. Hayden, J.H. Welsh, P.R. Levison, P.R. Shearing, D.G. Bracewell, Packed bed compression visualisation and flow simulation using an erosion-dilation approach, Journal of Chromatography A, 1611 (2020) 460601.
[17] R.A. Shalliker, V. Wong, B.S. Broyles, G. Guiochon, Visualization of bed compression in an axial compression liquid chromatography column, Journal of Chromatography A, 977 (2002) 213-223.
[18] R.A. Shalliker, B.S. Broyles, G. Guiochon, Physical evidence of two wall effects in liquid chromatography, Journal of Chromatography A, 888 (2000) 1-12.
[19] A.E. Reising, S. Schlabach, V. Baranau, D. Stoeckel, U. Tallarek, Analysis of packing microstructure and wall effects in a narrow-bore ultrahigh pressure liquid chromatography column using focused ion-beam scanning electron microscopy, Journal of Chromatography A, 1513 (2017) 172-182.
[20] S. Bruns, U. Tallarek, Physical reconstruction of packed beds and their morphological analysis: Core–shell packings as an example, Journal of Chromatography A, 1218 (2011) 1849-1860.
[21] T. Müllner, K.K. Unger, U. Tallarek, Characterization of microscopic disorder in reconstructed porous materials and assessment of mass transport-relevant structural descriptors, New Journal of Chemistry, 40 (2016) 3993-4015.
[22] A.J. Sederman, P. Alexander, L.F. Gladden, Structure of packed beds probed by Magnetic Resonance Imaging, Powder Technology, 117 (2001) 255-269.
[23] U. Tallarek, E. Baumeister, K. Albert, E. Bayer, G. Guiochon, NMR imaging of the chromatographic process migration and separation of bands of gadolinium chelates, Journal of Chromatography A, 696 (1995) 1-18.
[24] U. Tallarek, E. Bayer, D. Van Dusschoten, T. Scheenen, H. Van As, G. Guiochon, U.D. Neue, Dynamic NMR microscopy of chromatographic columns, AIChE Journal, 44 (1998) 1962-1975.
[25] S. Bruns, D. Stoeckel, B.M. Smarsly, U. Tallarek, Influence of particle properties on the wall region in packed capillaries, Journal of Chromatography A, 1268 (2012) 53-63.
[26] A.E. Reising, J.M. Godinho, J.W. Jorgenson, U. Tallarek, Bed morphological features associated with an optimal slurry concentration for reproducible preparation of efficient capillary ultrahigh pressure liquid chromatography columns, Journal of Chromatography A, 1504 (2017) 71-82.
[27] D. Hlushkou, U. Tallarek, Analysis of microstructure–effective diffusivity relationships for the interparticle pore space in physically reconstructed packed beds, Journal of Chromatography A, 1581-1582 (2018) 173-179.

[28] S. Bruns, J.P. Grinias, L.E. Blue, J.W. Jorgenson, U. Tallarek, Morphology and Separation Efficiency of Low-Aspect-Ratio Capillary Ultrahigh Pressure Liquid Chromatography Columns, Analytical Chemistry, 84 (2012) 4496-4503.
[29] S. Bruns, E.G. Franklin, J.P. Grinias, J.M. Godinho, J.W. Jorgenson, U. Tallarek, Slurry concentration effects on the bed morphology and separation efficiency of capillaries packed with sub-2 μm particles, Journal of Chromatography A, 1318 (2013) 189-197.
[30] A. Martinez, M. Kuhn, H. Briesen, D. Hekmat, Enhancing the X-ray contrast of polymeric biochromatography particles for three-dimensional imaging, Journal of Chromatography A, 1590 (2019) 65-72.
[31] A. dos Santos Pereira, A.J. Girón, E. Admasu, P. Sandra, Green hydrophilic interaction chromatography using ethanol–water–carbon dioxide mixtures, Journal of Separation Science, 33 (2010) 834-837.
[32] F. Gritti, Y. Kazakevich, G. Guiochon, Measurement of hold-up volumes in reverse-phase liquid chromatography: Definition and comparison between static and dynamic methods, Journal of Chromatography A, 1161 (2007) 157-169.
[33] A.E. Reising, S. Schlabach, V. Baranau, D. Stoeckel, U. Tallarek, Analysis of packing microstructure and wall effects in a narrow-bore ultrahigh pressure liquid chromatography column using focused ion-beam scanning electron microscopy, J Chromatogr A, 1513 (2017) 172-182.
[34] J.E. Baur, E.W. Kristensen, R.M. Wightman, Radial dispersion from commercial high-performance liquid chromatography columns investigated with microvoltammetric electrodes, Analytical Chemistry, 60 (1988) 2334-2338.
[35] J.E. Baur, R.M. Wightman, Microcylinder electrodes as sensitive detectors for high-efficiency, high-speed liquid chromatography, Journal of Chromatography A, 482 (1989) 65-73.

Figure Captions

Fig. 1. (A) The partial extruded silica/polymer rod (ID. 4.6 mm, Length=45 mm) of immobilized silica particles, (B) the polished sample for SEM imaging, and (C) Magnified cross-section image showing the maximum thickness of the wall region and the area of bulk region.[34, 35]

Fig. 2. Representative isocratic HILIC test chromatograms obtained on both columns in 92%/8% ACN/ammonium formate buffer (pH = 6.4) as mobile phase with a flow rate of 0.6 mL/min (= optimal velocity).

Fig. 3. Cropped square SEM images of two HPLC columns, and 4 slices for each column are randomly chosen to count the proportion of silica (the area of silica particles were outlined).

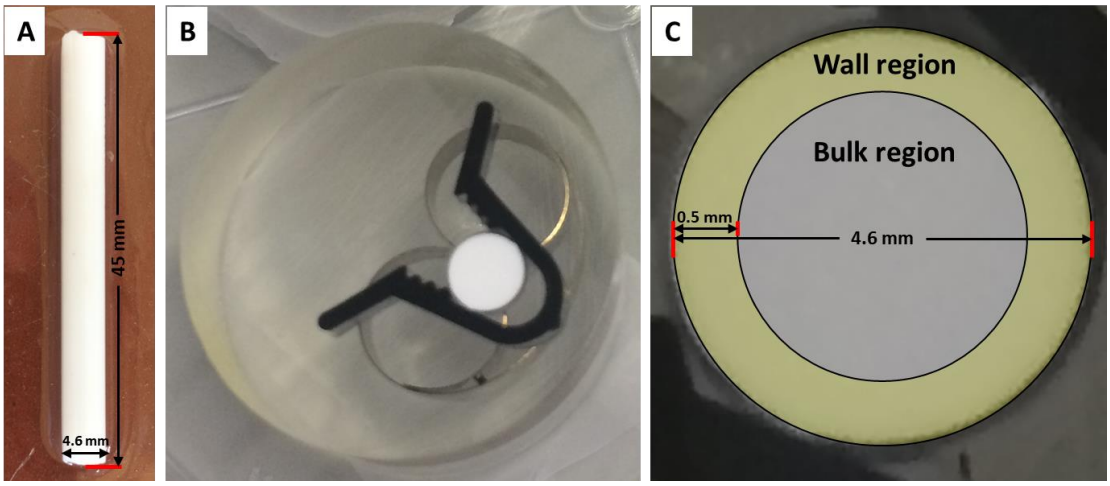

Figure 1

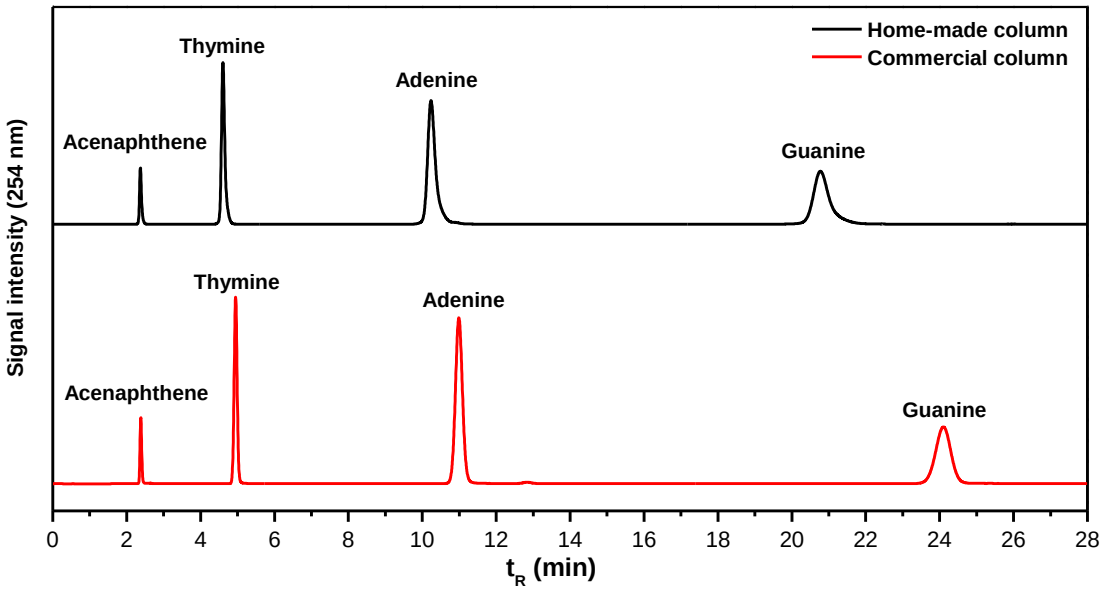
Home-made column
Commercial column
Thymine
Adenine
Acenaphthene
Guanine
Thymine
Adenine
Acenaphthene
Guanine
Signal intensity (254 nm)
0
2
4
6
8
10
12
14
16
18
20
22
24
26
28
t_R (min)

Figure 2

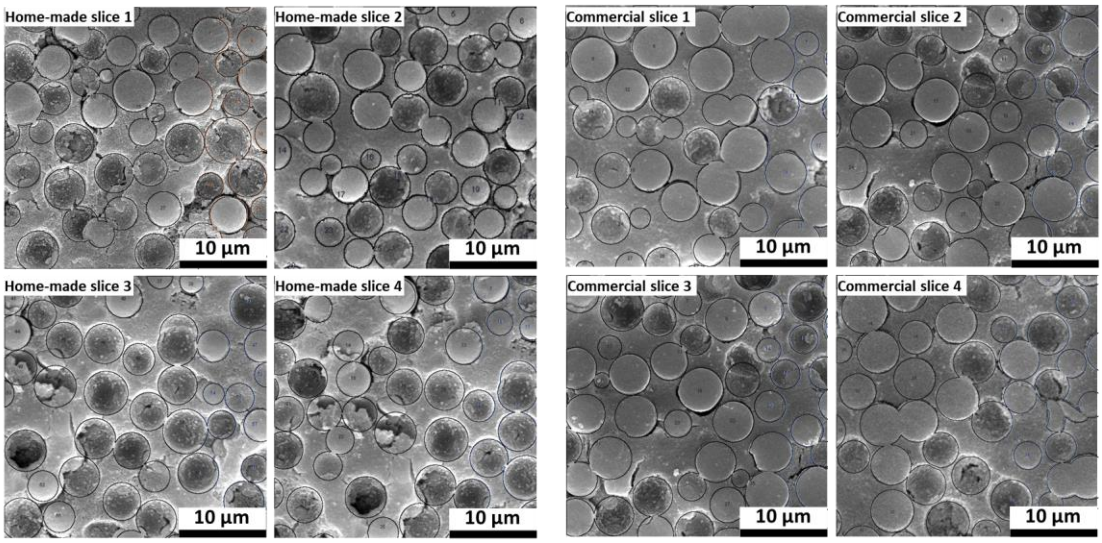
Home-made slice 1
10 µm
Home-made slice 2
10 µm
Commercial slice 1
10 µm
Commercial slice 2
10 µm
Home-made slice 3
10 µm
Home-made slice 4
10 µm
Commercial slice 3
10 µm
Commercial slice 4
10 µm

Figure 3

Table 1. Overview of the total and external porosity values measured via the various techniques on each column. (VD = determined from the elution time of the t_0-marker (acenaphthene) at 1 mL/min during the data collection for the construction of the Van Deemter curves; Pycno=determined via pycnometry measurements; ISEC = obtained from inversed size exclusion measurements; SEM = calculated from the statistical proportion of silica in the SEM images).

Columns	ε_T (VD)	ε_T (Pycno)	ε_e (ISEC@0.4mL/min)	ε_e (ISEC@0.8 mL/min)	ε_e (SEM)
Home-made	56.98%	65.70%	42.87%±0.12%	43.23%±0.26%	43.28%±2.67%
ZORBAX RX-SIL	57.31%	67.20%	41.98%±0.13%	41.97%±0.07%	39.10%±0.75%

Table 2. % coverage of the silica in 4 randomly selected square images (slices) together with the averaged values. The slices are represented in Figure 3. The column on the right represents the corresponding interstitial void volume fraction (= 100 – Average value) also represented in Table 1 (right column).

Columns	Slice 1	Slice 2	Slice 3	Slice 4	Average	RSD	Void volume fraction
Home-made	58.37%	57.59%	55.80%	55.12%	56.72%	2.67%	43.28%
Commercial	60.36%	60.68%	61.22%	61.33%	60.90%	0.75%	39.1%

Through-pore polymerization in polar high-performance liquid chromatography columns allowing scanning electron microscopy based imaging of the packing order

Supplementary Information:

Zhanyao Hou[a], Ken Broeckhoven[b], Gert Desmet[b], Frederic Lynen[a]*

a. Separation Science Group, Department of Organic and Macromolecular Chemistry, Faculty of Sciences, Ghent University, Krijgslaan 281-S4 Bis, B-9000 Ghent, Belgium.

b. Vrije Universiteit Brussel, Department of Chemical Engineering, Pleinlaan 2, Brussel, Belgium.

*Corresponding Author.

Tel: +32 (0) 9 264 9606; Fax: +32 (0) 9 264 4998. E-mail: frederic.lynen@ugent.be (F. Lynen)

S1. Column porosity definitions

Porosity is defined as the fraction of non-solid space in a certain volume element. In liquid chromatography, porosity is used to quantify the space in the column that is accessible to the mobile phase. Customarily, column porosity is composed of total, external and internal porosities. The total porosity (ε_T) is related to the total open voids (V_0) to which the mobile phase can access (through pore voids and inner pore voids), and the external porosity (ε_e) refers only to the through pore voids. The internal porosity (ε_{int}) is the volumetric fraction of the pores in the particles, corresponding to the ratio of the volume of inner pore voids to the geometrical volume of the particle ($V_{particle}$)

$$\varepsilon_t = \frac{V_{through\ pore}+V_{inner\ pore}}{V_G} \quad \text{(eq. S1)}$$

$$\varepsilon_e = \frac{V_{through\ pore}}{V_G} \quad \text{(eq. S2)}$$

$$\varepsilon_{int} = \frac{V_{inner\ pore}}{V_{particle}} = \frac{V_{inner\ pore}}{V_G \cdot (1-\varepsilon_e)} = \frac{\varepsilon_t - \varepsilon_e}{1-\varepsilon_e} \quad \text{(eq. S3)}$$

Where V_G is the column geometrical volume, calculated as $V_G = \pi \times r^2 \times L$.

S2. Total column porosity measurements

The total porosity of the column was assessed in two ways. In the first approach this was assessed *via* the dead volumes obtained from the elution time of an unretained marker (acenaphthene) during the van Deemter experiments described in the manuscript. The corresponding ε_T values as reported in table 1 were obtained *via* triplicate injections at 1 mL/min.

$$\varepsilon_T = \frac{V_0}{V_G} = \frac{t_0 \times F}{V_G} \quad \text{(eq. S4)}$$

Where V_0 is the void volume of the column (mL), F is volumetric flow rate (mL/min) and t_0 is the elution time at the apex of the acenaphthene peak.

In the second approach pycnometric measurements were performed using THF (ρ=0.8876 g/mL) and dichloromethane (ρ=1.3266 g/mL) as pure liquids, respectively.[1] the hold-up volume, V_0, is thereby calculated from density of each solvent (represented by ρ) and from the measured total weights of the column (m_{THF} and m_{CH2Cl2}) obtained when filling with THF and dichloromethane, respectively:

$$V_0 = \frac{m_{CH_2Cl_2} - m_{THF}}{\rho_{CH_2Cl_2} - \rho_{THF}} \quad \text{(eq. S5)}$$

Whereby ρ represents the density of each solvent.

S3. Inversed size exclusion methodology used for the determination of the external column porosity

External porosity values (ε_e) were measured experimentally by inverse size exclusion chromatography (ISEC) using a set of twelve polystyrene standards (MW=500; 2000; 3000; 10,000; 20,000; 30,000; 70,000; 150,000; 300,000; 700,000; 1000,000; 2000,000). Each standard was dissolved in a concentration of 1 mg/mL in pure tetrahydrofuran. The eluent was THF of which the flow rate was set at 0.4 mL/min and 0.8 mL/min. Injection volumes were 6 µL and the detection wavelength was 254 nm. Each injection was performed in triplicate. Retention volumes (obtained by multiplying the measured elution times with the flow rate) were corrected for the extra-column volumes of the system. The elution volumes of the polystyrene standards were subsequently plotted against the logarithm of the molecular mass of the polystyrene standards corresponding to the peak maximum as specified by the supplier.

S4. Column efficiency evaluation protocol

A mobile phase consisting of ACN and ammonium formate (NH_4HCO_3) buffer (92%/8%; v/v) was used for the efficiency evaluations of both columns. The interstitial velocity u_i was utilized for plotting van Deemter curves.

$$u_i = \frac{F}{\varepsilon_e \pi r^2} \qquad \text{(eq. S6)}$$

Where F is the mobile phase flow rate.

Plate heights were measured for at least 10 different velocities on both columns to construct van Deemter curves. All the reported plate height data was obtained after correction for the system band broadening (σ^2_{sys}) and dead time (t_{sys}) determined by removing the column from the system and replacing it with a zero dead-volume connector under same experimental conditions as for the plate height measurements.

$$N_{col} = \frac{(t_{R,total} - t_{R,sys})^2}{\sigma^2_{total} - \sigma^2_{sys}} \qquad \text{(eq. S7)}$$

$$H_{col} = \frac{L}{\mathrm{N}_{col}} \qquad \text{(eq. S8)}$$

In which, the subscript “total” refers to the experimentally measured efficiency, analysis time; the subscript “col” refers to the column efficiency obtained after correction.

Plate height data were subsequently fitted to the van Deemter equation:

$$H_{col} = A + \frac{B}{u_i} + C u_i \qquad \text{(eq. S9)}$$

Where A, B and C are the eddy diffusion, longitudinal dispersion and resistance to mass transfer coefficients, respectively.

S5. Column efficiency data

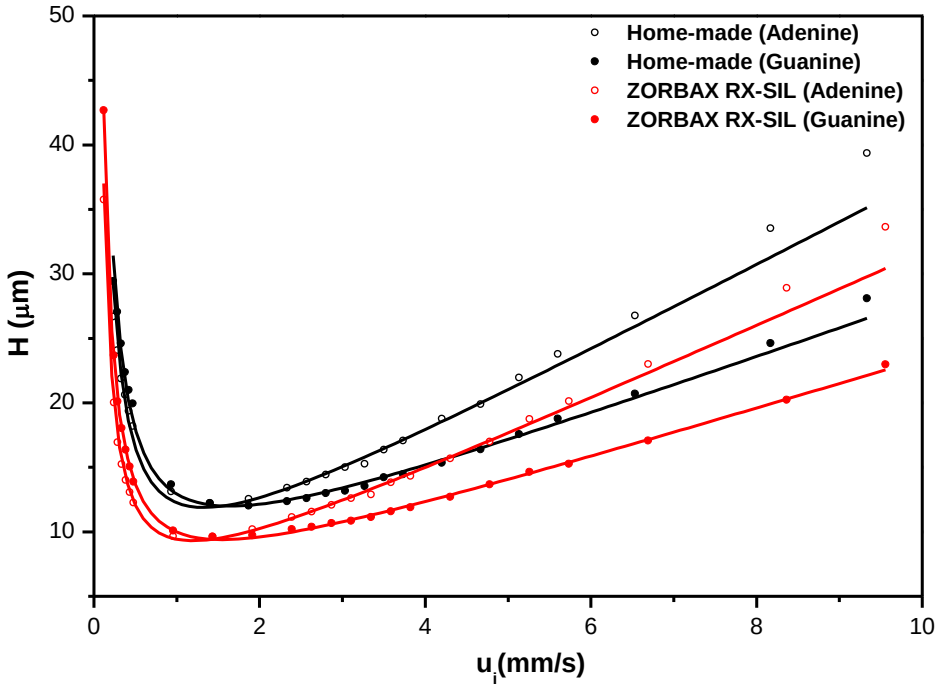

Fig. S1. Obtained Van Deemter plots representing the plate height (H) versus the interstitial velocity (u_i) for two test molecules on the repacked (○: Adenine; ●: Guanine) and on the commercial (○: Adenine; ●: Guanine) column.

Table S1. The symmetry factor and retention factor of the last two test molecules obtained on both columns in 92%/8% ACN/ammonium formate buffer (pH = 6.4) as mobile phase with a flow rate of 0.6 mL/min (= optimal velocity). Note: The symmetry factor is calculated as the ratio of front to back width at 10% of peak height.

Columns	Symm (1)	Symm (2)	*K'*(1)	*K'*(2)
Home-made column	0.67	0.72	3.3	7.8
Commercial column	0.92	1.03	3.6	9.2

1. Adenine; 2. Guanine

Table S2. Obtained van Deemter coefficients from curves fitting for two columns.

Columns	A^1	B^1	C^1	$u_{i,opt}$ (mm/s)	H^1_{min}(µm)	A^2	B^2	C^2	$u_{i,opt}$(mm/s)	H^2_{min} (µm)
Home-made	2.90	5.97	3.39	1.34	11.89	4.47	6.17	2.29	1.61	11.99
ZORBAX RX-SIL	2.45	4.09	2.88	1.17	9.32	3.34	4.68	1.96	1.55	9.40

1. Adenine; 2. Guanine

S6. External porosity data obtained via inversed size exclusion chromatography (ISEC)

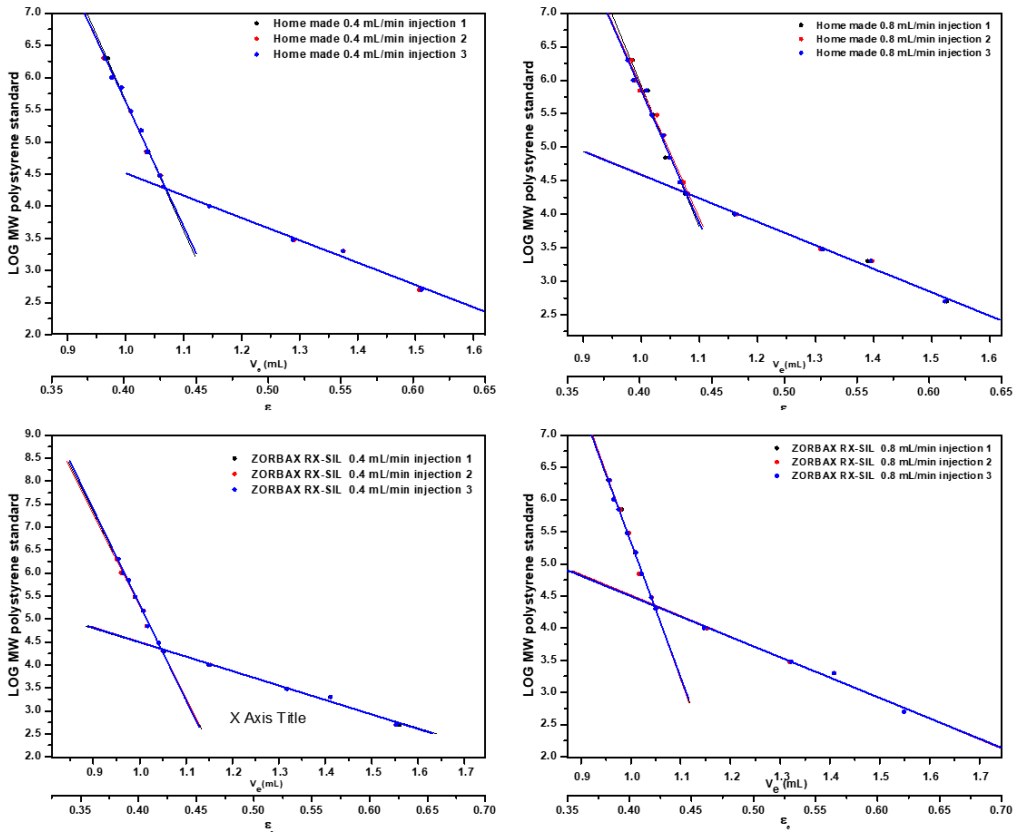

Fig. S2. ISEC plots obtained by separately injecting 12 different polystyrene standards on two columns at different flow rate (0.4 mL/min and 0.8 mL/min).

S7. Chemistry of the polymer

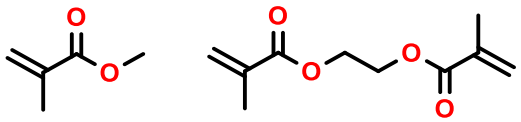

MMA **EGDMA**

Scheme S1. The chemical structures of monomer and cross-liner for in-column polymerization.

S8. Influence of the polishing process on the SEM imagery

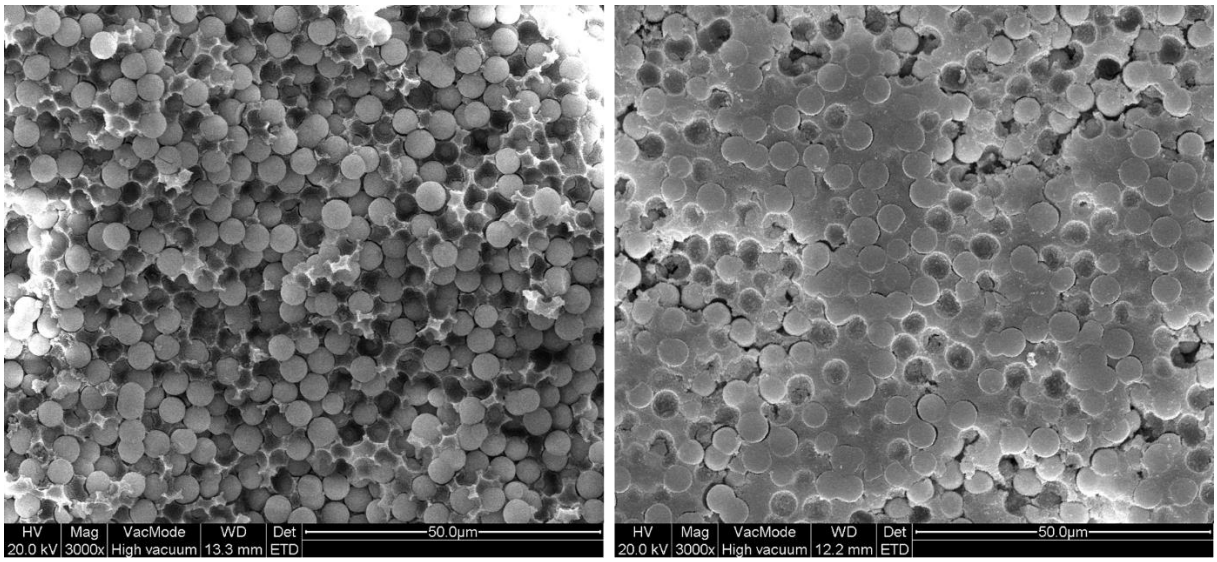

Fig. S3. An example of a comparison of micrographs obtained for a commercial column before (left) and after (right) the polishing process.

S9. Procedure used for SEM image processing

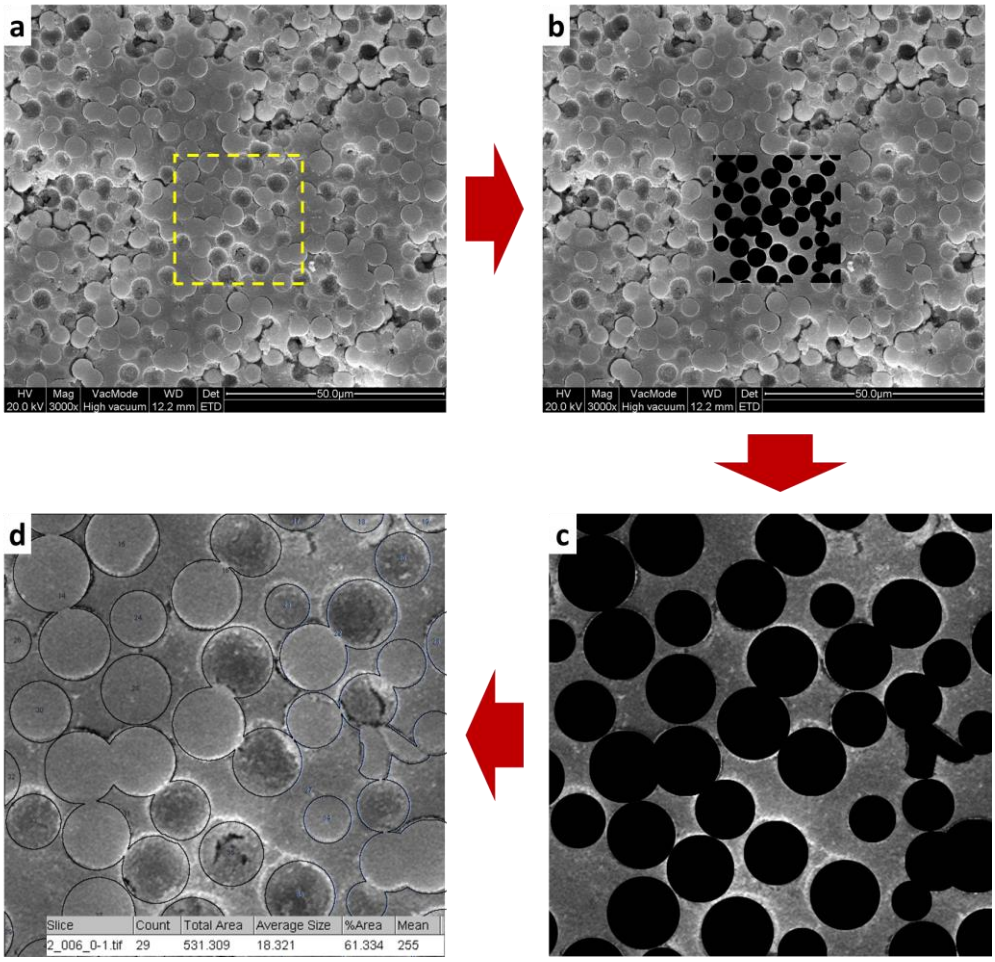

Fig. S4. An example of SEM image processing procedure: (a). Original SEM image and the selected appropriate square box (30 x 30 µm) pending for processing; (b). Highlighting the silica particles and cavities resulting from the loss of silica particles in black to enhance the contrast with the polymer area; (c) Cropping the highlighted square box; (d) Analyzing the proportion of the highlighted area by ImageJ software of which the result is shown in insert image.

References

[1] J.S. Baker, J.C. Vinci, A.D. Moore, L.A. Colón, Physical characterization and evaluation of HPLC columns packed with superficially porous particles, Journal of Separation Science, 33 (2010) 2547-2557.